

CHEMISTRY

A European Journal

A Journal of



Accepted Article

Title: Anomeric 5-Aza-7-deaza-2'-deoxyguanosines in Silver Ion Mediated Homo and Hybrid Base Pairs: Impact of Mismatch Structure, Helical Environment and Nucleobase Substituents on DNA Stability

Authors: Xinglong Zhou, Dasharath Kondhare, Peter Leonard, and Frank Seela

This manuscript has been accepted after peer review and appears as an Accepted Article online prior to editing, proofing, and formal publication of the final Version of Record (VoR). This work is currently citable by using the Digital Object Identifier (DOI) given below. The VoR will be published online in Early View as soon as possible and may be different to this Accepted Article as a result of editing. Readers should obtain the VoR from the journal website shown below when it is published to ensure accuracy of information. The authors are responsible for the content of this Accepted Article.

To be cited as: *Chem. Eur. J.* 10.1002/chem.201901276

Link to VoR: <http://dx.doi.org/10.1002/chem.201901276>

Supported by
ACES

WILEY-VCH

**Anomeric 5-Aza-7-deaza-2'-deoxyguanosines in Silver Ion Mediated Homo and Hybrid
Base Pairs: Impact of Mismatch Structure, Helical Environment and Nucleobase
Substituents on DNA Stability**

Xinglong Zhou,^[a] Dasharath Kondhare,^[a] Peter Leonard,^[a] and Frank Seela*^[a,b]

^[a] *Laboratory of Bioorganic Chemistry and Chemical Biology, Center for Nanotechnology,
Heisenbergstrasse 11, 48149 Münster, Germany,* ^[b] *Laboratorium für Organische und
Bioorganische Chemie, Institut für Chemie neuer Materialien, Universität Osnabrück,
Barbarastrasse 7, 49069 Osnabrück, Germany*

Corresponding author:

Prof. Dr. Frank Seela

Phone: +49 (0)251 53 406 500; Fax: +49 (0)251 53 406 857

E-mail: Frank.Seela@uni-osnabrueck.de

Homepage: www.seela.net

Supporting information for this article is available on the www under

<http://dx.doi.org/10.1002/chem.2016xxxx>.

Accepted Manuscript

Abstract

Nucleoside configuration (α -D vs β -D), nucleobase substituents and the helical DNA environment of silver-mediated 5-aza-7-deazaguanine-cytosine base pairs have a strong impact on DNA stability. This is the result of investigations performed on oligonucleotide duplexes with silver-mediated base pairs of α -D and β -D anomeric 5-aza-7-deaza-2'-deoxyguanosines and anomeric 2'-deoxycytidines incorporated in 12-mer duplexes. To this end, a new synthesis protocol was developed to access the pure anomers of 5-aza-7-deaza-2'-deoxyguanosine by glycosylation of either the protected nucleobase or its salt followed by separation of glycosylation products by crystallization and chromatography. Thermal stability measurements were performed on duplexes with α -D/ α -D and β -D/ β -D homo base pairs or α -D/ β -D and β -D/ α -D hybrid pairs within two sequence environments - positions 6 or 7 - of oligonucleotide duplexes. The individual T_m stability increase observed after silver ion addition differs significantly. Homo base pairs with β -D/ β -D or α -D/ α -D nucleoside combination were more stable than α -D/ β -D hybrid base pairs. The positional switch of silver ion mediated base pairs has a significant impact on the stability. Nucleobase substituents introduced at the 5-position of the dC site of silver-mediated base pairs effect base pair stability to a minor extent. Our investigation might find application in the construction of bioinspired nanodevices, in DNA diagnostics or metal DNA hybrid materials.

Introduction

The DNA double helix as carrier of genetic information uses a four letter code system.

Nucleoside dA forms a Watson-Crick base pair with dT and dG with the complementary dC.^[1]

The base pairs are held together by hydrogen bonds leading to a less stable bidentate dA-dT pair and more stable tridentate dG-dC pair.

More than 50 years ago,^[2] it was recognized that silver ions interact with DNA and several binding motifs were proposed including those with silver ions replacing protons within the Watson-Crick pairs. More recently, detailed information was collected regarding structure and stability of silver-mediated base pairs by various laboratories including ours. The formation of silver-mediated dC-dC base pair was established by single-crystal X-ray analyses.^[3] A series of publications appeared and reviews are available.^[4,5]

Multiple incorporations of silver ions in DNA can form “metal” DNA in which all canonical base pairs are replaced by silver-mediated pairs.^[4b,e,f] By this means nanoscopic silver wires can be constructed which have the potential to conduct electrons through the DNA molecule. Other applications for silver-mediated base pairs is their use in DNA diagnostics for the detection of mismatches in nucleic acids.^[5d]

In principle, the programmable replacement of a H-bonded Watson-Crick base pair by a silver-mediated pair is encountered with problems resulting from the presence of canonical base pairs. Consequently, DNA mismatches were introduced to destabilize DNA at a particular site. Then, silver ion binding is directed to the destabilized region. However, the amount of added silver ion equivalents should be in the range of the mismatches. The dC-dC mismatch and the formation of a silver-mediated dC-Ag-dC pair is a typical example for this phenomenon. If the amount of silver ions is considerably increased not only mismatches but also canonical H-bonded Watson-Crick base pairs form silver-mediated pairs. This occurs in a non-programmable way resulting in the formation of DNA silver wires.^[4b,f]

Recently, we reported on a silver-mediated base pair formed by 5-aza-7-deaza-2'-deoxyguanosine (**1**, β -dZ) with dC^[6] (purine numbering is used throughout the manuscript). The modified purine nucleoside **1**^[7] combines structural elements of dG and 7-deaza-dG (c^7G_d) and represents a shape mimic of the canonical nucleoside. Similar to 7-deaza-dG, 5-aza-7-deaza-dG cannot form Hoogsteen base pairs due to the lack of nitrogen-7. Different from dG and c^7G_d , nitrogen-1 of **1** is now an acceptor site for protons and silver ions. Consequently, the dZ-dC pair forms a mismatch and a metal ion mediated base pair in the presence of silver ions. This dZ-dC pair represents a silver-mediated purine-pyrimidine pair that closely mimics the canonical dG-dC pair.

In previous publications, we have shown that the silver-mediated α -dC/ β -dC hybrid pair is more stable than the β -dC-Ag⁺- β -dC homo pair^[8]. The terms “homo” and “hybrid” correspond solely to the stereochemistry at the anomeric center. Such a phenomenon let us anticipate that a similar behavior might exist in the silver-mediated dZ-dC pair. To study this matter on oligonucleotide duplexes, considerable amounts of stereochemically pure α -D and β -D-anomers of dZ (**1** and **2**) have to be available. Unfortunately, the chemical synthesis of the pure 5-aza-7-deaza-2'-deoxyguanosine α - and β -anomers **1** and **2** (Figure 1) is cumbersome as pure anomers are not formed by the widely used stereoselective nucleobase anion glycosylation.^[7b] Also, the almost identical mobilities of anomers makes the separation of the anomeric mixture difficult.

To this end, the nucleobase glycosylation of the 5-aza-7-deazaguanine base with the Hoffer halogenose **7**^[9] was reinvestigated with the intention to improve the formation of one particular anomer during the glycosylation reaction. Thereafter, 12-mer oligonucleotides were synthesized from corresponding phosphoramidites incorporating combinations of the anomeric nucleosides **1-4** (Figure 1). Oligonucleotides were hybridized in the absence and the presence of silver ions and the base pair stability was verified by T_m measurements. The anomeric silver-mediated base pairs were introduced at two different positions of the DNA double helix to probe nearest

neighbor influences and the impact of DNA helical environment on the helix stability. This includes studies regarding the influence of space demanding substituents introduced in the dC part of the anomeric dZ-dC base pairs.

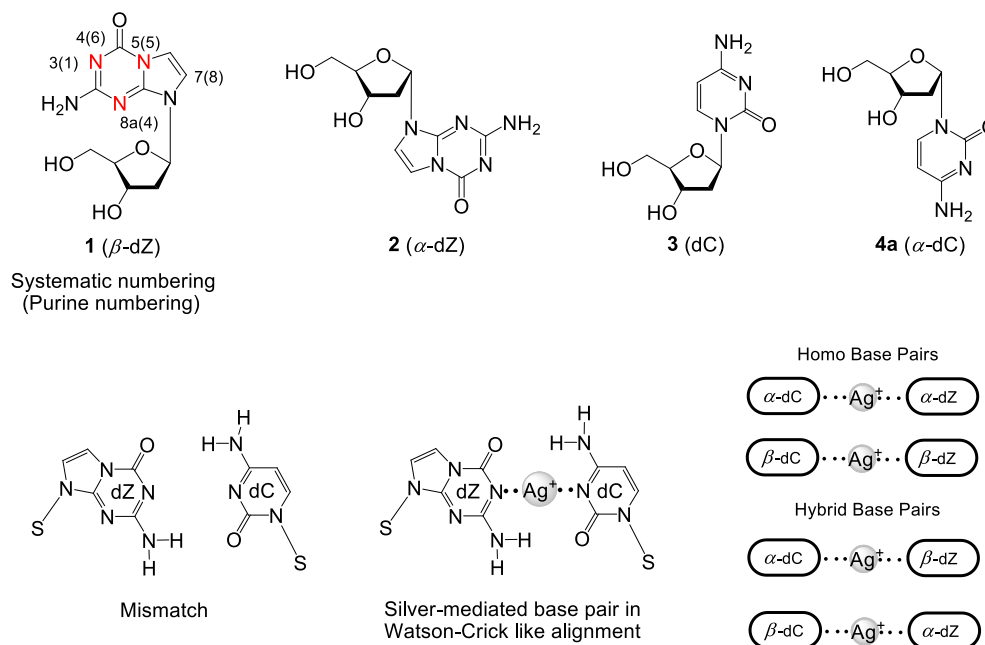


Figure 1. Upper part: Anomeric 5-aza-7-deaza-2'-deoxyribonucleosides β -dZ (**1**) and α -dZ (**2**) and anomeric dC nucleosides **3** and **4a**. Lower part left: Mismatch and silver-mediated base pair. Lower part right: Schematic view of silver-mediated homo and hybrid base pairs studied in this work.

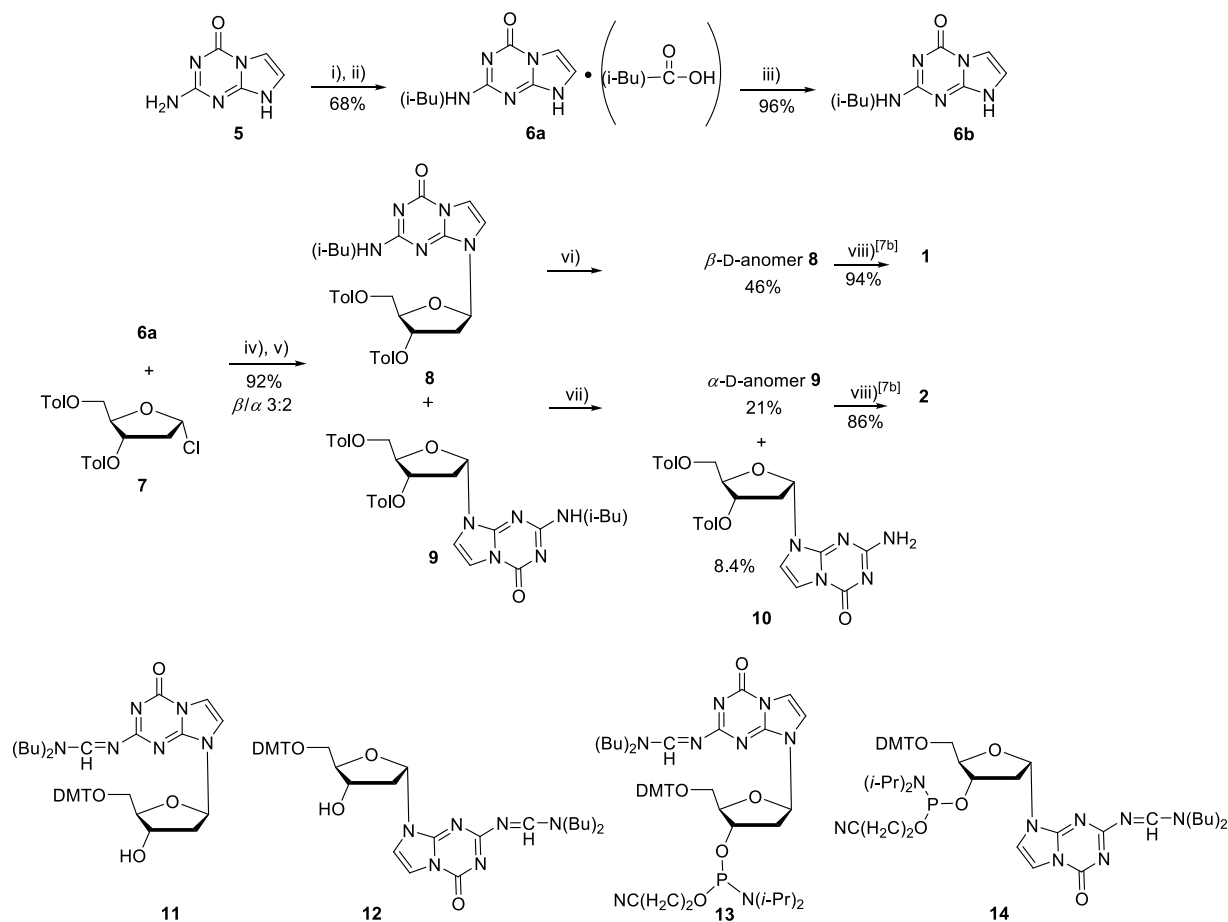
Results and Discussion

Synthesis and characterization of monomers

Earlier, both anomeric nucleosides **1** and **2** were synthesized by nucleobase anion glycosylation of the isobutyryl protected 5-aza-7-deazapurine **5**^[7b,1] utilizing the halogenose **7** (Hoffer sugar).^[9] However, the α -D anomer **9** was the favored species and not the β -D anomer **8** as observed for purines and 7-deazapurines. Therefore, attempts were made to shift the anomeric ratio of the

glycosylation reaction. Serendipitously, we found that glycosylation forms predominantly the β -D-anomer when the isobutyric acid salt **6a** is used instead of the free base **6b**. In detail, after isobutyrylation the salt **6a** was precipitated from the acidic reaction mixture and was used without further recrystallization. The salt structure of **6a** was confirmed by ^1H NMR spectra showing signals for two isobutyryl groups (Figure S9, Supporting Information).

Next, glycosylation was performed in MeCN, with TDA-1 and anhydrous potassium carbonate utilizing a two-fold excess of the halogenose **7**. Purification of the reaction mixture from by-products by flash chromatography without separation of the anomers resulted in 92% yield of an anomeric mixture of **8/9**. The ratio of anomers determined by ^1H NMR spectroscopy was 3:2 (β -D to α -D). The column pre-purified anomeric reaction mixture was crystallized from MeOH yielding the pure β -D nucleoside **8** in 46% yield. The content of the mother liquor was chromatographed yielding the pure α -nucleoside **9** in 21% together with 8% of the deprotected α -D anomer **10**. This method represents so far the most efficient way to obtain both anomers in sufficient yields using a combination of crystallization (β -anomer) and chromatography (α -anomer) (Scheme) (for details, see Experimental Section). The phosphoramidites **13** and **14**^[7f] as well as the phosphoramidites **15a-c** and **16a-c**^[8b] were prepared as described (for structures see Figure 3, Supporting Information).



Scheme. Upper part: Synthesis of protected nucleobase residues and nucleobase-anion glycosylation protocol for the synthesis of β -dZ (**1**) and α -dZ (**2**). i) $(i\text{-Bu})_2\text{O}$, H_3PO_4 , reflux; ii) precipitation from the reaction mixture; iii) recryst. aq. MeOH; iv) TDA-1, MeCN, K_2CO_3 , r.t., 1h, v) flash column (FC); vi) recryst. from aq. MeOH; vii) FC of the mother liquor; viii) sat. NH_3/MeOH . Lower part: Protected 5-aza-7-deaza-2'-deoxyguanosine nucleoside derivatives used in this study.

All compounds were characterized by mass spectra and high resolution ^1H , ^{13}C NMR and 2D NMR spectra (Figures S9-S84, Supporting Information). The UV spectra of the salt **6a** and the pure base **6b** show identical UV maxima at 224 and 278 nm and the molar extinction coefficients of both compounds are almost equal (14100 for **6a** and 13600 for **6b**, both measured at 278 nm). The isobutyrylated nucleobase **6b** shows two pK_a values: 3.1 for protonation and 7.7 for

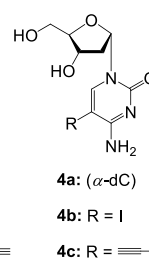
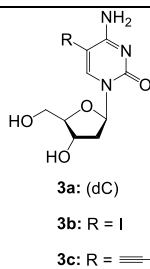
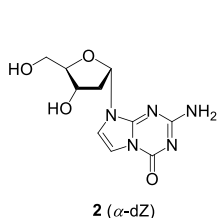
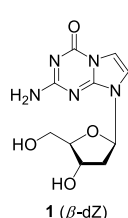
deprotonation, whereas the anomeric nucleosides show identical pK_a values only for protonation at $pK_a = 3.8$. (Table S1, Figures S1, S2, Supporting Information).

Synthesis and characterization of oligonucleotides

Next, oligonucleotides were prepared employing solid-phase synthesis using the phosphoramidites of α - and β -dZ^[7f] (**13**, **14**; Scheme) and of α - and β -dC^[8b] (Figure S3, Supporting Information) together with standard building blocks. The 5-aza-7-deazaguanine α - and β -anomers **1** (β -dZ) and **2** (α -dZ) were incorporated at two different positions of the 12-mer duplex 5'-d(TAGGTCAATACT) (ODN-1) • 3'-d(ATC CAG TTA TGA) (ODN-2) replacing a dA-dT (Table 2) or dG-dC (Table 3) base pair. ODN-1 • ODN-2 represents the well-characterized standard duplex of our laboratory and has been used to study a series of nucleoside analogues. After solid-phase synthesis, the oligonucleotides were cleaved from the solid support and deprotected in concentrated 28% aqueous ammonia at 55 °C for 2 h and then at rt overnight followed by purification by HPLC. Oligonucleotides incorporating anomeric dC residues with and without functionalization of the base were prepared according to the literature.^[8b] All oligonucleotides used for this study and their masses are shown in Table 1.

Table 1. Synthesized oligonucleotides and their molecular masses determined by MALDI-TOF mass spectrometry.^[a]

Entry	Oligonucleotides	M_r calcd. ^[a] M_r found ^[b]	Entry	Oligonucleotides	M_r calcd. ^[a] M_r found ^[b]
ODN-3	5'-d(TAGGTC2ATACT)	3661.4 3661.0	ODN-19	5'-d(TAGGT2AATACT)	3685.4 3685.4
ODN-4	5'-d(AGTAT4aGACCTA) ^[8b]	3630.4 3631.2	ODN-20	5'-d(AGTATT4aACCTA) ^[8b]	3603.6 3603.3
ODN-5	5'-d(AGTAT4bGACCTA) ^[8b]	3756.3 3754.8	ODN-21	5'-d(AGTATT4bACCTA) ^[8b]	3730.3 3730.2
ODN-6	5'-d(AGTAT4cGACCTA) ^[8b]	3734.5 3734.5	ODN-22	5'-d(AGTATT4cACCTA) ^[8b]	3709.5 3709.3
ODN-7	5'-d(TAGGTC4bATACT) ^[8b]	3747.3 3746.9	ODN-23	5'-d(TAGGT4bAATACT) ^[8b]	3770.3 3771.1
ODN-8	5'-d(AGTAT2GACCTA)	3670.4 3670.4	ODN-24	5'-d(AGTATT2ACCTA)	3645.4 3646.0
ODN-9	5'-d(TAGGTC4cATACT) ^[8b]	3725.5 3725.9	ODN-25	5'-d(TAGGT4cAATACT) ^[8b]	3749.6 3749.3
ODN-10	5'-d(TAGGTC1ATACT)	3661.4 3661.0	ODN-26	5'-d(AGTATT3aACCTA) ^[8b]	3605.4 3604.4
ODN-11	5'-d(AGTAT1GACCTA)	3670.4 3669.8	ODN-27	5'-d(AGTATT3bACCTA) ^[8b]	3730.3 3730.5
ODN-12	5'-d(AGTAT3aGACCTA) ^[8b]	3630.4 3631.1	ODN-28	5'-d(AGTATT3cACCTA) ^[8b]	3709.5 3710.1
ODN-13	5'-d(AGTAT3bGACCTA) ^[8b]	3756.3 3756.7	ODN-29	5'-d(TAGGT3bAATACT) ^[8b]	3770.3 3770.5
ODN-14	5'-d(AGTAT3cGACCTA) ^[8b]	3734.5 3734.1	ODN-30	5'-d(TAGGT3cAATACT) ^[8b]	3749.6 3748.3
ODN-15	5'-d(TAGGTC3bATACT) ^[8b]	3747.3 3747.2	ODN-31	5'-d(TAGGT1AATACT) ^[8a]	3685.4 3684.2
ODN-16	5'-d(TAGGTC3cATACT) ^[8b]	3725.5 3724.2	ODN-32	5'-d(AGTATT1ACCTA) ^[8a]	3645.2 3642.7



[a] Calculated on the basis of the molecular mass of $[M + H]^+$. [b] Determined by MALDI-TOF mass-spectrometry as $[M + H]^+$ in the linear positive mode.

Silver-mediated base pair formation

Recent studies on silver-mediated α -dC/ β -dC hybrid base pairs^[8] showed that very stable silver-mediated duplexes are formed when one nucleoside in the base pair shows α -D configuration and the other is the β -D anomer. As it was anticipated that the phenomenon is of general

applicability, this work studies now silver-mediated anomeric dZ-dC hybrid base pairs and base pair stability was compared with silver-mediated β -D/ β -D and α -D/ α -D homo pairs.

It became obvious that significant differences exist among silver-mediated base pairs of dZ with dC and those of dC with dC. In the latter case, both nucleobases are identical and the two pyrimidine moieties form a silver-mediated base pair that is slimmer than the corresponding purine-pyrimidine Watson-Crick pair. On the contrary, the size of the silver-mediated dZ-dC pair is close to that of the canonical dG-dC pair. Furthermore, the X-ray structure of the dC-Ag-dC pair^[3a] teaches us that in canonical DNA the nucleobases are in a *cisoid* alignment. However, in the methylated base derivatives *cisoid* and *transoid* alignments have been reported.^[4e,10] The orientation of the dZ-Ag-dC base pair can be Watson-Crick like or reverse Watson-Crick like. For the formation of a silver-mediated base pair, the stability of the silver-free mismatch plays an important role. Promiscuous base pairing and dependence on rigidity or flexibility of nearest neighbors segments have to be considered as well. Thus, the final increase of the helix stability generated by a silver-mediated base pair depends on a number of factors caused by the mismatch and the silver-ion mediated base pair within duplex DNA.

Figure 2 shows typical melting profiles of three selected duplexes in the absence and presence of silver ions. In all cases, thermodynamically stable silver-mediated 5-aza-7-deazaguanine - cytosine base pairs were formed indicated by a significant increase of T_m values. In order to demonstrate the specificity of the process sodium bromide was added to the buffer solution. Bromide ions can capture silver ions from the silver-mediated base pair and turn the metal pair back to a silver ion free mismatch.^[5i] The recovery of the initial melting profiles after halide addition are shown in Figures 2a,c,d confirming the reactivation of the silver ion free duplex and the stabilization by silver ions. Stoichiometric titration experiments are used to confirm the consumption of silver-ion equivalents per base pair (Figure 2b).

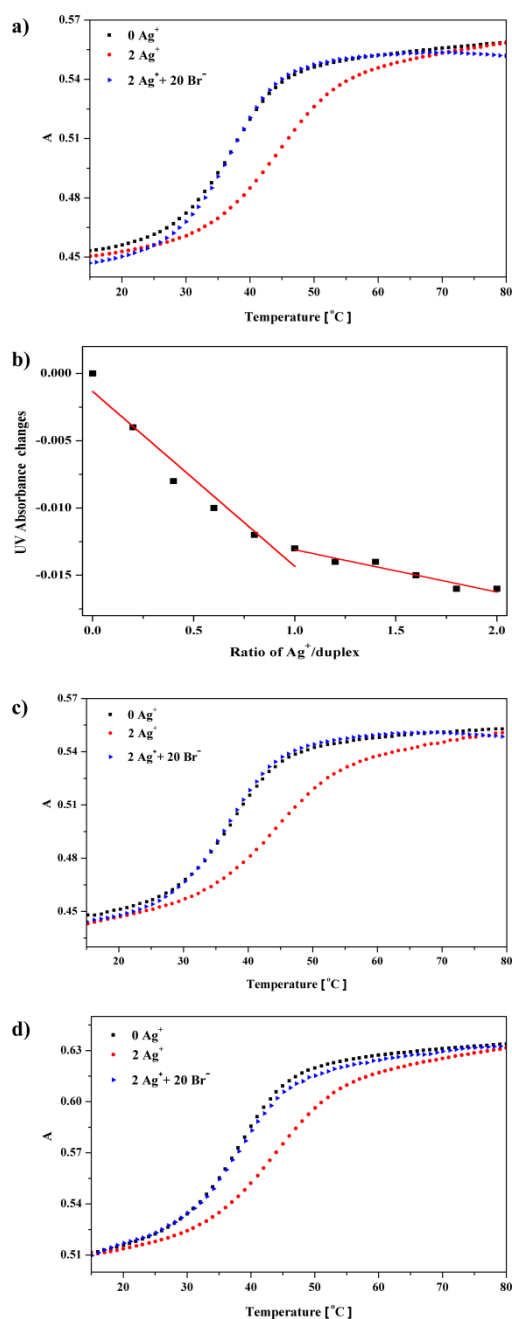


Figure 2. Thermal denaturation curves were measured at 2.5 μM + 2.5 μM single-strand concentration in 100 mM NaOAc, 10 mM $\text{Mg}(\text{OAc})_2$, pH 7.4 at 260 nm in the absence (black curves) and presence of two equivalents of Ag^+ -ions (red curves) followed by addition of 20 eq. of NaBr (blue curve). a) 5'-d(TAGGTC2AT ACT) (ODN-3) • 3'-d(ATCCAG4aTATGA) (ODN-4); c) 5'-d(TAGGTC2ATACT) (ODN-3) • 3'-d(ATCCAG4bTATGA) (ODN-5); d) 5'-d(TAG GTC2ATACT) (ODN-3) • 3'-d(ATCCAG4cTATGA) (ODN-6); b) titration graph displaying consumption of silver ions/duplex versus changes in UV absorbance (measured at 260 nm) for duplex ODN-3 • ODN-4. All duplexes contain α -D/ α -D homo base pairs.

In the following silver-mediated base pair stability was studied using temperature dependent melting of mismatch DNA in the absence and presence of silver ions (Tables 2 and 3). Homo and hybrid base pairs were investigated. The homo base pairs were either β -D/ β -D or α -D/ α -D pairs whereas in the series of hybrid base pairs either the α -anomer of dZ paired with β -dC or the β -anomer of dZ base pairs with α -dC. Furthermore, the positional impact of silver-mediated base pair formation was examined by shifting the metal ion base pair from position-7 to position-6. Also, the impact of space demanding residues (iodo, octadiynyl) located at the 5-position of dC was evaluated with regard to a possible functionalization without disturbing the helical DNA structure.

The T_m increase induced by silver ions was then used to establish silver-mediated base pair formation. Table 2 and 3 summarize T_m data for mismatches incorporated in the standard duplex ODN-1•ODN-2. In Table 2, a dA-dT base pair at position-7 was replaced by silver-mediated base pairs, whereas in Table 3 a dG-dC base pair at position-6 was substituted by the silver ion pair. All experiments were performed under identical conditions in a 100 mM NaOAc, 10 mM Mg(OAc)₂ buffer at pH 7.4 and were measured at 260 nm in the absence and the presence of silver ions. Single-strand concentration was 2.5 μ M. All curves show sigmoidal melting profiles and no or very little hysteresis.

Table 2 shows T_m data for duplexes with dZ-dC mismatches at position-7 of the duplex in the presence and the absence of silver ions. The upper part of the Table 2 displays homo pairs with α -D/ α -D mismatches (left) and β -D/ β -D mismatches (right). The lower part of the Table shows T_m data for α -D/ β -D hybrid pairs under participation of the α -dZ anomer **2** (left) and the β -dZ anomer **1** (right). A significant T_m increase was observed for α -dZ (**2**) in base pairs with α -dC (homo pairs) or β -dC (hybrid pairs), whereas duplexes with β -dZ did not show any significant T_m increase after silver ion addition, neither in homo pairs nor in hybrid pairs (right side of Table 2). For the β -D/ β -D homo pairs the small stability increase might be explained by the high stability

of the silver-free mismatches. These mismatches are too stable to complex silver ions; a situation which is similar to the standard duplex that does not form silver-mediated base pairs under the same conditions. However, this explanation does not hold for the hybrid pairs.

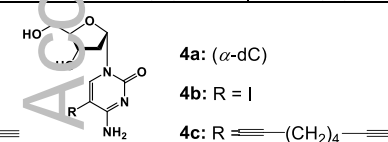
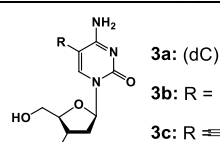
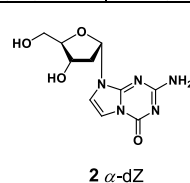
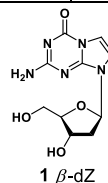
Furthermore, stability changes were observed when nucleoside residues in mismatches were reversed (duplex **3•5** vs duplex **7•8**). Thus, in the homo base pairs a positional impact of the various dZ-dC silver pairs exists when the 5-aza-7-deazapurine nucleoside is moved from one strand to the other. It should also be noted that the side chain modifications at the dC site have an influence on the mismatch stability. This is shown for base pairs containing 5-iodo-2'-deoxycytidines (**3b**, **4b**) or 5-octadiynyl-2'-deoxycytidines (**3c**, **4c**) with anomeric sugar configurations. 5-Iodo and 5-octadiynyl substituents introduced at the dC side of the homo base pairs have only a small impact on stability in the presence or absence of silver ions. On the contrary, for the hybrid base pairs the situation is more complex. In case of the β -D/ α -D hybrid pair even a destabilizing effect is observed which is more pronounced for the 5-iodo substituent than for the 5-octadiynyl side chain.

Table 2. T_m values of oligonucleotide duplexes containing α/α - and β/β -homo base pairs and α/β -hybrid base pairs of anomeric dZ nucleosides (**1** and **2**) with anomeric dC residues (**3a-c** and **4a-c**) in the presence and absence of silver ions replacing a dA-dT base pair (position-7).^[a]

Duplexes	T_m value [°C]	T_m value [°C] +1Ag ⁺ / duplex (ΔT_m [°C])	T_m value [°C] +2Ag ⁺ / duplex (ΔT_m [°C])	Duplexes	T_m value [°C]	T_m value [°C] +1Ag ⁺ / duplex (ΔT_m [°C])	T_m value [°C] +2Ag ⁺ / duplex (ΔT_m [°C])
α -D/ α -D Homo Pairs				β -D/ β -D Homo Pairs			
				5'-d(TAG GTC AAT ACT) (ODN-1) 3'-d(ATC CAG TTA TGA) (ODN-2)	47	48 (+1)	47 (±0)
5'-d(TAG GTC 2 AT ACT) (ODN-3) 3'-d(ATC CAG 4a TA TGA) (ODN-4)	36	41 (+5)	43 (+7)	5'-d(TAG GTC 1 AT ACT) (ODN-10) 3'-d(ATC CAG 3a TA TGA) (ODN-12)	38	40 (+2)	41 (+3)
5'-d(TAG GTC 2 AT ACT) (ODN-3) 3'-d(ATC CAG 4b TA TGA) (ODN-5)	36	41 (+5)	44 (+8)	5'-d(TAG GTC 1 AT ACT) (ODN-10) 3'-d(ATC CAG 3b TA TGA) (ODN-13)	40	41 (+1)	42 (+2)
5'-d(TAG GTC 2 AT ACT) (ODN-3) 3'-d(ATC CAG 4c TA TGA) (ODN-6)	37	40 (+3)	43 (+6)	5'-d(TAG GTC 1 AT ACT) (ODN-10) 3'-d(ATC CAG 3c TA TGA) (ODN-14)	40	40 (±0)	41 (+1)
5'-d(TAG GTC 4b AT ACT) (ODN-7) 3'-d(ATC CAG 2 TA TGA) (ODN-8)	35	39 (+4)	39 (+4)	5'-d(TAG GTC 3b AT ACT) (ODN-15) 3'-d(ATC CAG 1 TA TGA) (ODN-11)	40	42 (+2)	42 (+2)
5'-d(TAG GTC 4c AT ACT) (ODN-9) 3'-d(ATC CAG 2 TA TGA) (ODN-8)	36	40 (+4)	40 (+4)	5'-d(TAG GTC 3c AT ACT) (ODN-16) 3'-d(ATC CAG 1 TA TGA) (ODN-11)	42	43 (+1)	44 (+2)
α -D/ β -D Hybrid Pairs				β -D/ α -D Hybrid Pairs			
5'-d(TAG GTC 2 AT ACT) (ODN-3) 3'-d(ATC CAG 3a TA TGA) (ODN-12)	34	38 (+4)	39 (+5)	5'-d(TAG GTC 1 AT ACT) (ODN-10) 3'-d(ATC CAG 4a TA TGA) (ODN-4)	35	35 (±0)	34 (-1)
5'-d(TAG GTC 2 AT ACT) (ODN-3) 3'-d(ATC CAG 3b TA TGA) (ODN-13)	30	34 (+4)	36 (+6)	5'-d(TAG GTC 1 AT ACT) (ODN-10) 3'-d(ATC CAG 4b TA TGA) (ODN-5)	33	33 (±0)	32 (-1)
5'-d(TAG GTC 2 AT ACT) (ODN-3) 3'-d(ATC CAG 3c TA TGA) (ODN-14)	32	34 (+2)	36 (+4)	5'-d(TAG GTC 1 AT ACT) (ODN-10) 3'-d(ATC CAG 4c TA TGA) (ODN-6)	34	33 (-1)	32 (-2)
5'-d(TAG GTC 3b AT ACT) (ODN-15) 3'-d(ATC CAG 2 TA TGA) (ODN-8)	29	31 (+2)	31 (+2)	5'-d(TAG GTC 4b AT ACT) (ODN-7) 3'-d(ATC CAG 1 TA TGA) (ODN-11)	32	32 (±0)	32 (±0)
5'-d(TAG GTC 3c AT ACT) (ODN-16) 3'-d(ATC CAG 2 TA TGA) (ODN-8)	31	34 (+3)	33 (+2)	5'-d(TAG GTC 4c AT ACT) (ODN-9) 3'-d(ATC CAG 1 TA TGA) (ODN-11)	37	36 (-1)	36 (-1)

Position 1 3 5 7 9 11

5'-d(TAGGTC**2**AATACT) ODN-1
3'-d(ATCCAGTT**4a**TATGA) ODN-2



[a] Measured at 260 nm with 2.5 μM + 2.5 μM single-strand concentration at a heating rate of 1.0 °C/min in 100 mM NaOAc, 10 mM Mg(OAc)₂, pH 7.4 in the presence of various concentrations of AgNO₃ (0-2 eq. of silver ions/duplex). T_m values were calculated from the heating curves using the program Meltwin 3.0.^[11] $\Delta T_m = T_m$ after the addition of AgNO₃ – T_m before the addition of AgNO₃.

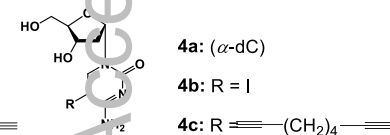
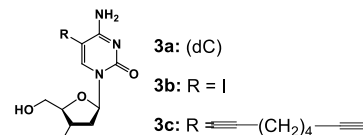
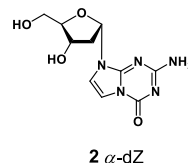
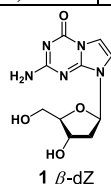
Next, mismatches were shifted from the 7-position to position-6 replacing a dG-dC pair of the double helix (Table 3). Now, the mismatches are surrounded by two dA-dT Watson-Crick pairs. In this position, the silver-free mismatches are less stable than those in position-7 (Table 2). This is the result from the loss of a dG-dC pair in this series compared to a dA-dT pair shown in the series of Table 2. In position-7, the most stable duplexes are formed by silver-mediated β -D/ β -D homo pairs, whereas α -D/ α -D pairs show significantly lower T_m increases. Also, hybrid pairs containing the α -dZ 2 show a T_m increase after silver ion addition. The higher T_m values of the β -d/ β -D homo base pairs compared to the α -D/ α -D homo and α -D/ β -D hybrid pairs result mainly from the higher stability of the silver-free mismatches. To visualize the rather complex situation bar diagrams were composed (Figure 3) summarizing the T_m values from Tables 2 and 3.

Table 3. T_m values of oligonucleotide duplexes containing α/α - and β/β -homo base pairs and α/β -hybrid base pairs of anomeric dZ nucleosides (**1** and **2**) with anomeric dC residues (**3a-c** and **4a-c**) in the presence and absence of silver ions replacing a dG-dC base pair (position-6).^[a]

Duplexes α -D/ α -D Homo Pairs	T_m value [°C]	T_m value [°C] +1Ag ⁺ / duplex (ΔT_m [°C])	T_m value [°C] +2Ag ⁺ / duplex (ΔT_m [°C])	Duplexes β -D/ β -D Homo Pairs	T_m value [°C]	T_m value [°C] +1Ag ⁺ / duplex (ΔT_m [°C])	T_m value [°C] +2Ag ⁺ / duplex (ΔT_m [°C])
				5'-d(TAG GTAAAT ACT) (ODN-17) 3'-d(ATC CAT TTATGA) (ODN-18)	42	42 (±0)	42 (±0)
5'-d(TAG GT 2 AAT ACT) (ODN-19) 3'-d(ATC CA 4a TTA TGA) (ODN-20)	25	28 (+3)	29 (+4)	5'-d(TAG GT 1 AAT ACT) (ODN-31) 3'-d(ATC CA 3a TTA TGA) (ODN-26)	30	37 (+7)	38 (+8)
5'-d(TAG GT 2 AAT ACT) (ODN-19) 3'-d(ATC CA 4b TTA TGA) (ODN-21)	24	27 (+3)	27 (+3)	5'-d(TAG GT 1 AAT ACT) (ODN-31) 3'-d(ATC CA 3b TTA TGA) (ODN-27)	30	33 (+3)	34 (+4)
5'-d(TAG GT 2 AAT ACT) (ODN-19) 3'-d(ATC CA 4c TTA TGA) (ODN-22)	26	28 (+2)	29 (+3)	5'-d(TAG GT 1 AAT ACT) (ODN-31) 3'-d(ATC CA 3c TTA TGA) (ODN-28)	29	32 (+3)	34 (+5)
5'-d(TAG GT 4a AAT ACT) (ODN-23) 3'-d(ATC CA 2 TTA TGA) (ODN-24)	25	27 (+2)	28 (+3)	5'-d(TAG GT 3b AAT ACT) (ODN-29) 3'-d(ATC CA 1 TTA TGA) (ODN-32)	35	37 (+2)	38 (+3)
5'-d(TAG GT 4c AAT ACT) (ODN-25) 3'-d(ATC CA 2 TTA TGA) (ODN-24)	25	29 (+4)	31 (+6)	5'-d(TAG GT 3c AAT ACT) (ODN-30) 3'-d(ATC CA 1 TTA TGA) (ODN-32)	31	33 (+2)	35 (+4)
α-D/β-D Hybrid Pairs				β-D/α-D Hybrid Pairs			
5'-d(TAG GT 2 AAT ACT) (ODN-19) 3'-d(ATC CA 3a TTA TGA) (ODN-26)	25	27 (+2)	29 (+4)	5'-d(TAG GT 1 AAT ACT) (ODN-31) 3'-d(ATC CA 4a TTA TGA) (ODN-20)	24	24 (±0)	24 (±0)
5'-d(TAG GT 2 AAT ACT) (ODN-19) 3'-d(ATC CA 3b TTA TGA) (ODN-27)	20	22 (+2)	23 (+3)	5'-d(TAG GT 1 AAT ACT) (ODN-31) 3'-d(ATC CA 4b TTA TGA) (ODN-21)	25	24 (-1)	22 (-3)
5'-d(TAG GT 2 AAT ACT) (ODN-19) 3'-d(ATC CA 3c TTA TGA) (ODN-28)	24	26 (+2)	28 (+4)	5'-d(TAG GT 1 AAT ACT) (ODN-31) 3'-d(ATC CA 4b TTA TGA) (ODN-22)	25	24 (-1)	24 (-1)
5'-d(TAG GT 3b AAT ACT) (ODN-29) 3'-d(ATC CA 2 TTA TGA) (ODN-24)	24	27 (+3)	27 (+3)	5'-d(TAG GT 4b AAT ACT) (ODN-23) 3'-d(ATC CA 1 TTA TGA) (ODN-32)	24	24 (±0)	24 (±0)
5'-d(TAG GT 3c AAT ACT) (ODN-30) 3'-d(ATC CA 2 TTA TGA) (ODN-24)	20	24 (+4)	25 (+5)	5'-d(TAG GT 4c AAT ACT) (ODN-25) 3'-d(ATC CA 1 TTA TGA) (ODN-32)	24	24 (±0)	24 (±0)

Position 1 4 6 8 10

5'-d(TAGGTCAATACT) ODN-1
3'-d(ATCCAGTTATGA) ODN-2



[a] Measured at 260 nm with 2.5 μM + 2.5 μM single-strand concentration at a heating rate of 1.0 °C/min in 100 mM NaOAc, 10 mM Mg(OAc)₂, pH 7.4 in the presence of various concentrations of AgNO₃ (0-2 eq. of silver ions/duplex). T_m values were calculated from the heating curves using the program Meltwin 3.0.^[11] $\Delta T_m = T_m$ after the addition of AgNO₃ - T_m before the addition of AgNO₃.

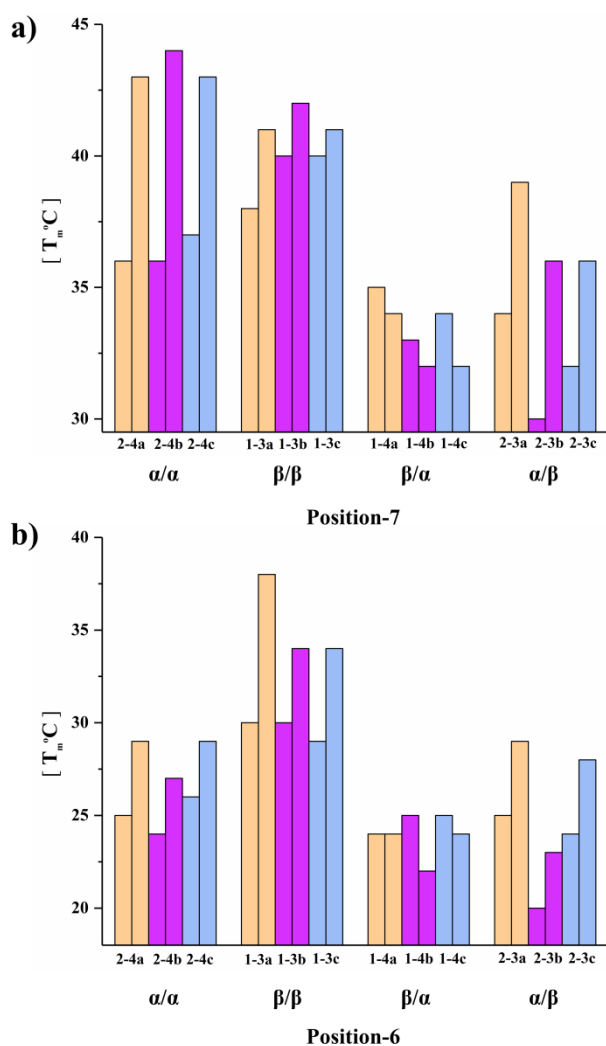


Figure 3. Bar diagrams of T_m values for DNA duplexes containing homo and hybrid base pairs of anomeric dZ (**1,2**) with anomeric 5-substituted dC (**3a-c,4a-c**) in the absence (first bar) and presence (second bar) of silver ions according to Tables 2 and 3. a) 5'-d(TAGGTCXATACT) • 3'-d(ATCCAGYTATGA) (7-position); b) 5'-d(TAGGTXAATACT) • 3'-d(ATCCAYTTATGA) (6-position).

From the figure the following conclusions can be drawn. Position-6: (i) the highest T_m increases and most stable silver-mediated base pairs are observed when both nucleosides display β -D configuration. (ii) The α -D/ α -D homo pairs are less stable and show reduced T_m

increases after silver ion addition. (iii) Strong T_m increases but less stable base pairs are observed for the hybrid pairs with dZ in α -configuration, whereas the β/α pairs becomes destabilized after silver ion addition.

Position-7: (i) the α/α combinations form the most stable silver-mediated base pairs and show significant T_m increases. (ii) The β/β pairs are significantly less stable and the T_m increase after silver addition is low. (iii) The α/β hybrid pairs are stabilized by silver ion addition, when dZ is in α -configuration, whereas destabilization is observed when β -dZ participates in the hybrid base pair. This is similar to position-6. Stability changes are also observed when the nucleobase is functionalized. The 5-iodo- and 5-octadiynyl substituents have a moderate but noticeable influence on mismatches and stability of silver-mediated DNA. However, these residues are in general well accommodated in the metal DNA. For the homo base pairs the effect of functionalization is almost negligible, whereas the situation is more complex in case of the hybrid base pairs. In presence of silver ions a destabilizing effect is observed which is more pronounced for the 5-iodo compared to the 5-octadiynyl substituent.

The global structure of DNA is extremely flexible and is able to accommodate distortions introduced by mismatches without altering the overall structure. On the local level the influence of mismatches can be moderate or strong. Taking into account that the stability of Watson-Crick base pairs and silver-free mismatches depends already on nearest neighbors^[12] or even on larger areas of the double helix, the stability of silver-mediated dZ-dC base pairs shows a similar behavior. The position of incorporation, the configuration of the nucleoside residue and modifications by substituents are of importance. The studies on homo and hybrid base pairs demonstrate that the helical DNA environment on both sides of a silver-mediated base pair has a significant impact on its stability. In principle, each combination of α - and β -anomers **1** and **2** with dC generates a particular mismatch and a corresponding silver-mediated base pair of unique stability.

A general stability increase induced by silver-mediated base pair formation is observed for almost each silver-mediated base pair at both positions (6- and 7-substitution). However, the individual T_m increases differ significantly. When already rather stable mismatches are formed in the absence of silver ions, the tendency to form thermodynamically stable silver-mediated base pairs is lower than in the case of low stability mismatches. Thus, the impact of the local environment of the silver-mediated base pair can vary from moderate to very extensive. Nevertheless, stability changes caused by substituents, configuration or nearest neighbors is different in silver-mediated base pair mismatches compared to Watson-Crick pairs.

It is also obvious, that the silver-mediated dZ-dC base pairs behave differently as the recently investigated anomeric dC-dC pairs.^[8] The distortion of the double helix by dC/dC mismatches is almost negligible, whereas local changes by purine-pyrimidine mismatches are more pronounced. In the latter cases, changes of the groove dimensions or breathing of the helix are more likely. Thus, it is difficult to predict structures for the various mismatches and silver-mediated base pairs. However, we anticipate that Watson-Crick like base pairs are formed in homo base pair interactions (α/α and β/β) according to Figure 4. The higher stability of these structures might be caused by the formation of one additional hydrogen bond, a phenomenon that was also reported for other silver-mediated base pairs.^[13] The formation of two hydrogen bonds is unlikely because to the size of the silver ion. In the less stable hybrid base pairs hydrogen bond formation is unlikely due to the possible reverse Watson-Crick like alignment of the nucleobases in the base pair (Figure 4). To this end DFT calculations^[14-17] were performed for the dZ-dC base pair containing one silver ion. The position of the silver ion was found to connect nitrogen-1 of the 5-aza-7-deazaguanine base with nitrogen-3 of the cytosine residue (Figure 4e). The silver-mediated base pair forms a Watson-Crick like motif. The dihedral angle $N1(9)-Ag-N3(4) = 159^\circ$ is not far from a linear connectivity. The

hydrogen of the amino group of the 5-aza-7-deazaguanine moiety and the oxo group of cytosine form an additional hydrogen bond ($\text{N-H}\dots\text{O} = 176^\circ$, $\text{H}\dots\text{O} = 2.11 \text{ \AA}$).

When the calculation started with the reverse Watson-Crick like motif of the silver-mediated dZ-dC pair the reverse structure collapsed during calculation to a Watson-Crick like structure. This confirms the low stability of the reverse Watson-Crick motif. Nevertheless, final answers on the individual structures of the silver-mediated base pairs cannot be given. The positional dependence of the base pair stability reported in this work indicates that the DNA environment surrounding the silver-mediated base pair has a strong impact on its stability, a phenomenon which is already known from silver-free DNA mismatches.^[12] This work also shows that the high stability of silver-free mismatches can impede silver-mediated base pair formation. Furthermore, it should be recalled that the DNA double helix backbone and therefore the position of incorporation might even alter the molecular structure of an individual silver-mediated base pair and base stacking has a significant impact on base pair stability.

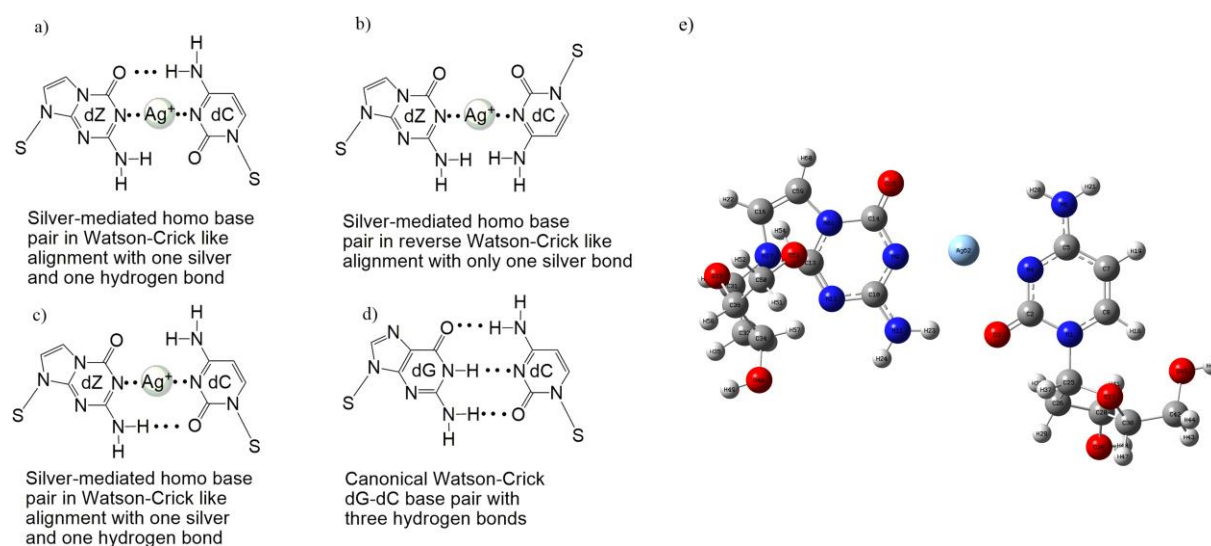


Figure 4. Silver-mediated base pairs with Watson-Crick like alignment and one hydrogen bond (a,c) or reverse Watson-Crick like alignment (b) and the canonical Watson-Crick dG-dC

base pair (d). Structure obtained from DFT calculations of the silver-mediated dZ-Ag⁺-dC pair (e). S corresponds to 2'-deoxyribofuranosyl sugar residues.

Conclusion

The stability of silver mediated base pairs of α -D and β -D anomeric 5-aza-7-deaza-2'-deoxyguanosines **1** and **2** with anomeric 2'-deoxycytidines **3** to **4** depends on nucleoside configuration, nucleobase substituents and the helical environment that surrounds the metal mediated DNA base pair. For this, the pure nucleoside anomers **1** and **2** were synthesized. Their access was significantly improved by the use of the isobutyrylated nucleobase **6b** or its salt **6a** for a particular anomer formed by nucleobase anion glycosylation. Efficient separation of anomeric glycosylation products was accomplished by combination of crystallization and chromatography. A series of phosphoramidites were prepared and used to synthesize 12-mer oligonucleotides with all four possible combinations of anomeric 5-aza-7-deaza-2'-deoxyguanosine and anomeric 2'-deoxycytidines. They were hybridized to form α -D/ α -D and β -D/ β -D homo base pairs as well as α -D/ β -D and β -D/ α -D hybrid pairs at position-6 or position-7 of duplex DNA. The individual stability of mismatches increases after silver ion addition and differs significantly between the various series. α -D/ β -D hybrid base pairs were less stable in this series, whereas homo base pairs with β/β or even α/α nucleoside combination form the most stable complexes. 5-Iodo and 5-octadiynyl substituents introduced at the dC side of the homo base pairs have only a small impact on stability while the situation is more complex for hybrid base pairs. In case of the β -D/ α -D hybrid pair even a destabilizing effect is observed, which is more pronounced for the 5-iodo derivatives than those with 5-octadiynyl side chain. The studies performed on silver-mediated homo and hybrid base pairs have the potential to be used for the development of new metal/DNA hybrid materials or as analytical tools for DNA diagnostics and detection.

Experimental Section

General methods and materials

All chemicals and solvents were of laboratory grade as obtained from commercial suppliers and were used without further purification. Reversed-phase HPLC was carried out using a HITACHI 655A-12 liquid chromatograph connected to L6200A intelligent pump and 655A variable wavelength UV monitor on a 4 x 250 mm RP-18 (10 μm) LiChrospher 100 column with a HPLC pump connected with a variable wavelength monitor, a controller and an integrator. The molecular masses of the oligonucleotides were determined by MALDI-TOF mass spectrometry on a Bruker Autoflex Speed in the linear positive mode with 3-hydroxypicolinic acid (3-HPA) as a matrix. The thermal melting curves were measured with an Agilent Technologies Cary 100 Bio UV-vis spectrophotometer equipped with a thermoelectrical controller. The temperature was measured continuously in the reference cell with a Pt-100 resistor with a heating rate of 1 $^{\circ}\text{C min}^{-1}$. T_m values were determined from the melting curves using the software MELTWIN, version 3.0.^[11]

Computational details

DFT calculations were used to optimize the molecular structure of the silver-mediated homo base pair. The calculation was performed using Gaussian 09^[14] program package with B3LYP-D3^[15] functional. The 6-311 G(d,p)^[16] and LANL2DZ^[17] basis sets were employed for light atoms (C, H, O, N) and Ag^+ -ion, respectively.

Oligonucleotide syntheses and characterization

Solid-phase oligonucleotide syntheses were performed on an ABI 392-08 synthesizer at 1 μmol scale (trityl-on mode) employing the phosphoramidites of α - and β -dZ,^[7f] (**13**, **14**; Scheme) and of α - and β -dC^[8b] (**15a-c**, **16a-c**; for structures see Figure S3 in the Supporting

Information) as well as the standard building blocks with an average coupling yield over 95%. After cleavage from the solid support, the oligonucleotides were deprotected in 28% aqueous ammonia at 55 °C for 2 h. The DMT-containing oligonucleotides were purified by reversed-phase HPLC (RP-18) with the gradient system at 260 nm: (A) MeCN, (B) 0.1 M (Et₃NH)OAc (pH 7.0)/MeCN, 95:5; gradient *I*: 0-3 min 10-15% A in B, 3-15 min 15-50% A in B; flow rate 0.7 mL/min. The purified “trityl-on” oligonucleotides were treated with 2.5% CHCl₂COOH/CH₂Cl₂ for 2 min at 0 °C to remove the 4,4'-dimethoxytrityl residues. The detritylated oligomers were purified again by reversed-phase HPLC with gradient *II*: 0-20 min 0-20% A in B; 20-25 min, 20% A in B; flow rate 0.7 mL/min. The oligonucleotides were desalted on a reversed-phase column (RP-18) using water for elution of salt, while the oligonucleotides were eluted with H₂O/MeOH (2:3). The oligonucleotides were lyophilized on a Speed-Vac evaporator to yield colorless solids which were frozen at -24 °C. The purity of all oligonucleotides was confirmed by RP-18 HPLC (Figure S4, Supporting Information) and MALDI-TOF mass spectrometry (Table 1). The extinction coefficients ϵ_{260} (H₂O) of the nucleosides are: dA 15400, dG 11700, dT 8800, dC 7300, β -dZ (**1**) 14100, α -dZ (**2**) 13700, (**3b**) 3100 (MeOH)^[8b], (**3c**) 5600 (MeOH)^[8b], (**4b**) 3400 (MeOH)^[8b], (**4c**) 5900 (MeOH)^[8b]. The extinction coefficients of the oligonucleotides were calculated from the sum of the extinction coefficients of nucleoside constituents.

2-[(2-Methylpropionyl)amino]-8H-imidazo[1,2-*a*]-s-triazin-4-one • ibuOH (6a).

2-Aminoimidazo[1,2-*a*]-s-triazin-4(8H)-one^[7a] (**5**) (1.5 g, 9.93 mmol) was suspended in isobutyric anhydride (35 mL). Then, two drops of 85% phosphoric acid were added to this solution and the reaction mixture was refluxed until the solution became clear (1.5 h). The reaction mixture was filtered and the remaining clear solution was stored at r.t. overnight. During this period the product precipitated. The precipitate was filtrated and washed by ice-

cold water (3 x 10 mL) furnishing compound **6a** as colorless solid (2.10 g, 68%). $R_f = 0.5$ ($\text{CH}_2\text{Cl}_2/\text{CH}_3\text{OH}$ 9:1); ^1H NMR (600 MHz, $[\text{D}_6]\text{DMSO}$, 26°C): $\delta = 12.51$ (bs, 1H; NH), 10.68 (bs, 1H; NH), 7.53 (d, $J = 1.3$ Hz, 1H; H-7), 7.38 (s, 1H; H-6), 2.82-2.86 (m, 1H; CH), 2.38-2.43 (m, 1H; CH), 1.04-1.07 ppm (m, 12H; CH_3); ^{13}C NMR (101 MHz, $[\text{D}_6]\text{DMSO}$, 26°C): $\delta = 18.91$ ($\text{CH}(\text{CH}_3)_2$), 19.05 ($\text{CH}(\text{CH}_3)_2$), 33.13 ($\text{CH}(\text{CH}_3)_2$), 37.80 ($\text{CH}(\text{CH}_3)_2$), 109.02 (C-7), 149.43 (C-8a), 177.84 (C=O); UV/Vis (CH_3OH): λ_{max} (ϵ) = 224 (18000), 278 nm (14100 $\text{mol}^{-1}\text{dm}^3\text{cm}^{-1}$); HRMS (ESI-TOF): m/z calcd for $\text{C}_9\text{H}_{11}\text{N}_5\text{O}_2\text{Na}$: 244.0805 [$M + \text{Na}$] $^+$; found 244.08025.

2-[(2-Methylpropionyl)amino]-8H-imidazo[1,2-a]-s-triazin-4-one (6b).^[7b] Compound **6a** (1.0 g, 3.23 mmol) was dissolved in 10% aq. MeOH (10 mL) by gentle warming. When the base was completely dissolved, the solution was immediately cooled to 0°C (ice-bath). After 10 min., white crystals appeared which were filtered and dried furnishing **6b** (410 mg, 57%). Evaporation of the mother liquor gave another crop of 275 mg (38%) of **6b**. The materials obtained from crystallization and evaporation of mother liquor were identical. $R_f = 0.5$ ($\text{CH}_2\text{Cl}_2/\text{CH}_3\text{OH}$ 9:1); ^1H NMR (600 MHz, $[\text{D}_6]\text{DMSO}$, 26°C): $\delta = 12.85$ (bs, 1H; NH), 10.65 (bs, 1H; NH), 7.53 (d, $J = 2.0$ Hz, 1H; H-7), 7.38 (s, 1H; H-6), 2.82-2.86 (m, 1H; CH), 1.06 ppm (d, $J = 6.9$ Hz, 6H; CH_3); ^{13}C NMR (101 MHz, $[\text{D}_6]\text{DMSO}$, 26°C): $\delta = 22.13$ ($\text{CH}(\text{CH}_3)_2$), 37.80 ($\text{CH}(\text{CH}_3)_2$), 112.1 (C-7), 152.95 (C-8a), 180.21 (C=O); UV/Vis (CH_3OH): λ_{max} (ϵ) = 224 (15900), 278 nm (13600 $\text{mol}^{-1}\text{dm}^3\text{cm}^{-1}$); HRMS (ESI-TOF): m/z calcd for $\text{C}_9\text{H}_{11}\text{N}_5\text{O}_2\text{Na}$: 244.0805 [$M + \text{Na}$] $^+$; found 244.08025.

Glycosylation of 2-aminoimidazo[1,2-a]-s-triazin-4(8H)-one • ibuOH (6b) with 2-deoxy-3,5-di-O-(p-toluoyl)- β -D-erythro-pentofuranosyl chloride (7). The nucleobase **6b** (0.50 mg, 1.62 mmol) was dissolved in dry CH_3CN (60 mL) under gentle warming. After cooling to r.t.

K_2CO_3 (996 mg, 3.6 mmol) and tris[2-(2-methoxyethoxy)ethyl]amine (100 μ L, 0.3 mmol) were added to the solution and stirring was continued for 20 min at rt. Then, the halogenose **7** (1.75 g, 4.52 mmol) was added in three portions over 10 min. Stirring at r.t. was continued until the base was completely consumed (1 h, TLC-monitoring). Then, the reaction mixture was filtrated and the solvent was evaporated. The remaining residue was dissolved in CH_2Cl_2 (5 mL) and applied to FC (silica gel, column 14 x 4 cm, $CH_2Cl_2/MeOH$ 100:0 \rightarrow 99:1). From the main zone a mixture of the anomers **8** and **9** (851 mg, 92%) in a ratio of 3/2 (β/α) was obtained as colorless foam. The anomeric ratio was calculated on the basis of the 1H NMR chemical shifts.

8-[2-Deoxy-3,5-di-O-(*p*-toluoyl)- β -D-erythro-pentofuranosyl]-2-[(2-methylpropionyl)

amino-8*H*-imidazo[1,2-*a*]-s-triazin-4-one (8**).^[7b] The anomeric mixture of **8** and **9** obtained**

by glycosylation (358 mg) was dissolved in MeOH (25 mL) by reflux for 2 min. While rapidly cooling the hot solution to r.t the β -D-anomer **8** crystallized as colorless needles.

Filtration and drying afforded β -D nucleoside **8** (428 mg, 46%). $R_f = 0.50$ (CH_2Cl_2/CH_3OH 95:5); 1H NMR (400 MHz, $[D_6]DMSO$, 26°C): $\delta = 10.39$ (s, 1H; NH), 7.93 (d, $J = 8.2$ Hz, 2H; Ar-H), 7.84 (d, $J = 8.2$ Hz, 2H; Ar-H), 7.72 (d, $J = 2.8$ Hz, 1H; H-6), 7.62 (d, $J = 2.7$ Hz, 1H; H-7), 7.37 (d, $J = 8.0$ Hz, 2H; Ar-H), 7.29 (d, $J = 8.0$ Hz, 2H; Ar-H), 6.41 (t, $J = 7.0$ Hz, 1H; H-1'), 5.78 (dt, $J = 6.6, 2.6$ Hz, 1H; H-3'), 4.65-4.51 (m, 3H; H-4', H-5'), 3.25-3.17 (m, 1H; H $_{\beta-2'}$), 2.94-2.85 (m, 1H; CH), 2.73 (d, $J = 18.0$ Hz, 1H; H $_{\alpha-2'}$), 2.40, 2.36 (s, 6H; Ar- CH_3), 1.04 ppm (d, $J = 6.8$ Hz, 6H; $CH(CH_3)_2$); 1H NMR (600 MHz, $CDCl_3$, 26°C): $\delta = 8.09$ (s, 1H; NH), 7.95 (d, $J = 8.2$ Hz, 2H; Ar-H), 7.86 (d, $J = 8.2$ Hz, 2H, Ar-H), 7.37 (d, $J = 2.7$ Hz, 1H; H-6), 7.28 (d, $J = 8.4$ Hz, 2H; Ar-H), 7.23 (d, $J = 8.0$ Hz, 2H; Ar-H), 7.11 (d, $J = 2.7$ Hz, 1H; H-7), 6.49-6.46 (m, 1H; H-1'), 5.74 (dt, $J = 5.1, 2.3$ Hz, 1H; H-3'), 4.76 (dd, $J = 11.5, 2.9$ Hz, 1H; H-4'), 4.66-4.60 (m, 2H; H-5'), 3.15-3.13 (m, 1H; H $_{\beta-2'}$), 2.91-2.81 (m, 2H; H $_{\alpha-2'}$

2', CH), 2.44, 2.41 (s, 6H; Ar-CH₃), 1.23 ppm (dd, $J = 6.9, 2.3$ Hz, 6H; CH(CH₃)₂); ¹³C NMR (101 MHz, [D₆]DMSO, 26°C): $\delta = 175.64$ (C=O), 165.39 (arom. C), 165.16 (arom. C), 160.72 (C-4), 149.94 (C-2), 149.40 (C-8a), 144.08 (arom. C), 143.78 (arom. C), 129.43 (arom. C), 129.32 (arom. C), 129.26 (arom. C), 129.23 (arom. C), 126.58 (arom. C), 126.48 (arom. C), 116.82 (C-7), 108.98 (C-6), 84.44 (C-1'), 81.92 (C-4'), 74.85 (C-3'), 64.06 (C-5'), 35.47 (CH(CH₃)₂), 35.46 (C-2'), 21.19, 21.15 (CH₃, (toluoyl)), 19.05, 19.03 (CH(CH₃)₂); UV/Vis (CH₃OH): $\lambda_{\max} (\epsilon) = 277$ (13800), 242 nm (37600 mol⁻¹dm³cm⁻¹); HRMS (ESI-TOF): m/z calcd for C₃₀H₃₁N₅O₇Na: 596.2116 [$M + H$]⁺; found 596.2115.

8-[2-Deoxy-3,5-di-O-(*p*-toluoyl)- α -D-erythro-pentofuranosyl]-2-[(2-methylpropionyl)amino-8*H*-imidazo[1,2-*a*]-s-triazin-4-one (9). ^[7b] The mother liquor obtained after

crystallization of the β -D-anomer **8** was evaporated and applied to FC (silica gel, column 14 x 4 cm, CH₂Cl₂/MeOH 100:0 \rightarrow 98:2). From the faster migrating zone the α -D anomer **9** was obtained (198 mg, 21%) as colorless foam. $R_f = 0.55$ (CH₂Cl₂/CH₃OH 95:5); ¹H NMR (400 MHz, [D₆]DMSO, 26°C): $\delta = 10.31$ (s, 1H; NH), 7.92 (d, $J = 8.2$ Hz, 2H; Ar-H), 7.72 (d, $J = 8.2$ Hz, 2H; Ar-H), 7.69 (d, $J = 2.7$ Hz, 1H; H-6), 7.60 (d, $J = 2.7$ Hz, 1H; H-7), 7.36 (d, $J = 8.0$ Hz, 2H; Ar-H), 7.28 (d, $J = 8.0$ Hz, 2H; Ar-H), 6.43 (t, 1H; H-1'), 5.60 (dt, $J = 5.3, 3.3$ Hz, 1H; H-3'), 5.06 (td, $J = 4.6, 2.4$ Hz, 1H; H-4'), 4.56-4.47 (m, 2H; H-5'), 2.99 (t, $J = 5.3$ Hz, 2H; H-2'), 2.91 (m, $J = 6.8$ Hz, 1H; CH), 2.37, 2.39 (s, 6H; Ar-CH₃), 1.05 ppm (d, $J = 6.8$ Hz, 6H; CH(CH₃)₂); ¹H NMR (600 MHz, CDCl₃, 26°C) $\delta = 8.43$ (s, 1H; NH), 7.91 (d, $J = 8.3$ Hz, 2H; Ar-H), 7.63 (d, $J = 8.3$ Hz, 2H; Ar-H), 7.46 (d, $J = 2.7$ Hz, 1H; H-6), 7.28 (d, $J = 2.7$ Hz, 1H; H-7), 7.25 (d, $J = 7.4$ Hz, 2H; Ar-H), 7.18 (d, $J = 7.9$ Hz, 2H; Ar-H), 6.50 (dd, $J = 6.7, 1.8$ Hz, 1H; H-1'), 5.63 (dt, $J = 6.4, 1.5$ Hz, 1H; H-3'), 4.86 (td, $J = 4.0, 1.6$ Hz, 1H; H-4'), 4.57 (d, $J = 4.1$ Hz, 2H; H-5'), 3.10-2.97 (m, 3H, H-2'; CH), 2.40, 2.37 (s, 6H; Ar-CH₃), 1.20 ppm (dd, $J = 6.9, 1.0$ Hz, 6H; CH(CH₃)₂); ¹³C NMR (101 MHz, [D₆]DMSO, 26°C): $\delta =$

175.66 (C=O), 165.47 (arom. C), 165.10 (arom. C), 160.59 (C-4), 150.01 (C-2), 148.56 (C-8a), 143.97 (arom. C), 143.91 (arom. C), 129.41 (arom. C), 129.34 (arom. C), 129.26 (arom. C), 129.22 (arom. C), 126.56 (arom. C), 126.39 (arom. C), 116.52 (C-7), 108.32 (C-6), 85.86 (C-1'), 83.54 (C-4'), 74.63 (C-3'), 64.01 (C-5'), 37.02 (C-2'), 34.58 (CH(CH₃)₂), 21.18 (CH₃, (toluoyl)), 19.13, 19.05 (CH(CH₃)₂); UV/Vis (CH₃OH): λ_{\max} (ϵ) = 280 (13100), 240 nm (39600 mol⁻¹dm³cm⁻¹); HRMS (ESI-TOF): m/z calcd for C₃₀H₃₁N₅O₇NNa: 596.2116 [$M + H$]⁺; found 596.2114.

2-Amino-8-[2-deoxy-3,5-di-*O*-(*p*-toluoyl)- α -D-erythro-pentofuranosyl]-8*H*-imidazo[1,2-*a*]-s-triazin-4-one (10). The mother liquor obtained after crystallization of the β -D-anomer **8** was evaporated and applied to FC (silica gel, column 14 x 4 cm, CH₂Cl₂/MeOH 100:0 →95:5). From the slower migrating zone compound **10** was obtained (78 mg, 8.4%) as colorless foam. R_f = 0.25 (CH₂Cl₂/CH₃OH 95:5); ¹H NMR (600 MHz, [D₆]DMSO, 26°C): δ = 7.91 (d, J = 8.2 Hz, 2H; Ar-H), 7.78 (d, J = 8.2 Hz, 2H; Ar-H), 7.44 (d, J = 2.8 Hz, 1H; H-6), 7.37 (d, J = 2.8 Hz, 1H; H-7), 7.35 (d, J = 8.0 Hz, 2H; Ar-H), 7.32 (d, J = 7.9 Hz, 2H; Ar-H), 6.94 (s, 2H, NH₂), 6.33 (dd, J = 7.1, 2.3 Hz, 1H; H-1'), 5.60 (dt, J = 6.9, 2.0 Hz, 1H; H-3'), 4.97-4.93 (m, 1H; H-4'), 4.51-4.45 (m, 2H; H-5'), 2.99 (dd, J = 14.6, 7.5 Hz, 1H; H $_{\beta}$ -2'), 2.77 (dt, J = 15.1, 1.9 Hz, 1H; H $_{\alpha}$ -2'), 2.38 ppm (d, J = 6.2 Hz, 6H; CH(CH₃)₂); ¹³C NMR (101 MHz, [D₆]DMSO, 26°C): δ = 175.66 (C=O), 165.47 (arom. C), 165.20 (C-4), 165.19 (arom. C), 149.93 (C-2), 149.63 (C-8a), 144.03 (arom. C), 143.95 (arom. C), 129.41 (arom. C), 129.34 (arom. C), 126.55 (arom. C), 126.40 (arom. C), 114.35 (C-7), 107.82 (C-6), 84.75 (C-1'), 83.35 (C-4'), 74.74 (C-3'), 64.08 (C-5'), 36.98 (C-2'), 21.19, 21.18 (CH₃, (toluoyl)); UV/Vis (CH₃OH): λ_{\max} (ϵ) = 243 nm (37900 mol⁻¹dm³cm⁻¹); HRMS (ESI-TOF): m/z calcd for C₂₆H₂₅N₅O₆H: 504.1878 [$M + H$]⁺; found 504.1869.

2-Amino-8-(2-deoxy- β -D-erythro-pentofuranosyl)-8H-imidazo[1,2a]-s-triazin-4-one (1).

^[7b] Compound **8** (1.15 g, 2.0 mmol) was suspended in NH₃/MeOH (150 mL) and the reaction mixture was stirred overnight until a clear solution was obtained. After evaporation of the solvent, the remaining residue was adsorbed on silica gel and applied to FC (silica gel, column 15 x 4 cm, CH₂Cl₂/MeOH 4:1). From the main zone compound **8** was obtained as colorless solid (520 mg, 94%). $R_f = 0.5$ (CH₂Cl₂/CH₃OH 4:1); ¹H NMR (600 MHz, [D₆]DMSO, 26°C): $\delta = 7.45$ (d, $J = 2.8$ Hz, 1H; H-7), 7.36 (d, $J = 2.8$ Hz, 1H; H-6), 6.94 (s, 2H; NH₂), 6.20-6.15 (m, 1H; H-1'), 5.29 (d, $J = 4.0$ Hz, 1H; 3'-OH), 4.97 (t, $J = 5.4$ Hz, 1H; 5'-OH), 4.32 (dq, $J = 6.3, 3.2$ Hz, 1H; H-3'), 3.83-3.79 (m, 1H; H-4'), 3.58-3.48 (m, 2H; H-5'), 2.38 (ddd, $J = 13.3, 7.6, 5.7$ Hz, 1H; H $_{\beta}$ -2'), 2.18 ppm (ddd, $J = 13.2, 6.1, 3.2$ Hz, 1H; H $_{\alpha}$ -2'); UV/Vis (CH₃OH): $\lambda_{\max} (\epsilon) = 258$ nm (14100 mol⁻¹dm³cm⁻¹). HRMS (ESI-TOF): m/z calcd for C₁₀H₁₃N₅O₄Na:290.0860 [$M + Na$]⁺; found 290.0863.

2-Amino-8-(2-deoxy- α -D-erythro-pentofuranosyl)-8H-imidazo[1,2a]-s-triazin-4-one (2).

^[7b] As described above with compound **9** (1.70 g, 3.0 mmol), NH₃/MeOH (150 mL). FC (silica gel, column 15 x 4 cm, CH₂Cl₂/MeOH 4:1) gave compound **2** as colorless solid (710 mg, 86 %). $R_f = 0.5$ (CH₂Cl₂/CH₃OH 4:1); ¹H NMR (600 MHz, [D₆]DMSO, 26°C): $\delta = 7.53$ (d, $J = 2.8$ Hz, 1H; H-7), 7.33 (d, $J = 2.8$ Hz, 1H; H-6), 6.97-6.83 (m, 2H; NH₂), 6.18 (dd, $J = 8.0, 2.5$ Hz, 1H; H-1'), 5.52 (d, $J = 3.4$ Hz, 1H; 3'-OH), 4.86 (t, $J = 5.6$ Hz, 1H; 5'-OH), 4.29 (dq, $J = 5.5, 2.3$ Hz, 1H; H-3'), 4.12-4.08 (m, 1H; H-4'), 3.43-3.39 (m, 2H; H-5'), 2.68 (ddd, $J = 14.4, 7.9, 6.6$ Hz, 1H; H $_{\beta}$ -2'), 2.11 ppm (dt, $J = 14.4, 2.3$ Hz, 1H; H $_{\alpha}$ -2'); UV/Vis (CH₃OH): $\lambda_{\max} (\epsilon) = 258$ (13700 mol⁻¹dm³cm⁻¹). HRMS (ESI-TOF): m/z calcd for C₁₀H₁₃N₅O₄Na:290.0860 [$M + Na$]⁺; found 290.0863.

Acknowledgements

We thank Dr. Simone Budow-Busse for critical reading of the manuscript. We would like to thank Dr. M. Letzel, Universität Münster, Germany, for the ESI-TOF spectra and Prof. Dr. B. Wunsch, Institut für Pharmazeutische und Medizinische Chemie, Universität Münster, Germany to provide us with 600 MHz NMR spectra. We thank Mrs. Oxana Korzhenko for the synthesis of oligonucleotides. We thank Prof. Dr. Jianping Hu, Sichuan Industrial Institute of Antibiotics, Chengdu University, China for the DFT calculation. Funding by ChemBiotech, Münster, Germany is gratefully acknowledged.

Conflict of interest

The authors declare no conflict of interest.

Key Words: DNA, 5-aza-7-deaza-2'-deoxyguanosine, silver ions, base pairing, duplex stability

References

- [1] J. D. Watson, F. H. C. Crick, *Nature* **1953**, *171*, 737-738.
- [2] a) T. Yamane, N. Davidson, *Biochim. Biophys. Acta* **1962**, *55*, 609-621; b) T. Yamane, N. Davidson, *Biochim. Biophys. Acta* **1962**, *55*, 780-782; c) R. H. Jensen, N. Davidson, *Biopolymers* **1966**, *4*, 17-32; d) M. Daune, C. A. Dekker, H. K. Schachman, *Biopolymers* **1966**, *4*, 51-76; e) G. L. Eichhorn, J. J. Butzow, P. Clark, E. Tarien, *Biopolymers* **1967**, *5*, 283-296; f) N. Dattagupta, D. M. Crothers, *Nucleic Acids Res.* **1981**, *9*, 2971-2985; g) R. M. Izatt, J. J. Christensen, J. H. Rytting, *Chem. Rev.* **1971**, *71*, 439- 481.

[3] a) J. Kondo, Y. Tada, T. Dairaku, H. Saneyoshi, I. Okamoto, Y. Tanaka, A. Ono, *Angew. Chem. Int. Ed.* **2015**, *54*, 13323–13326; b) H. Liu, F. Shen, P. Haruehanroengra, Q. Yao, Y. Cheng, Y. Chen, C. Yang, J. Zhang, B. Wu, Q. Luo, R. Cui, J. Li, J. Ma, J. Sheng, J. Gan, *Angew. Chem. Int. Ed.* **2017**, *129*, 9558-9562.

[4] a) Y. Takezawa, J. Müller, M. Shionoya, *Chem. Lett.* **2017**, *46*, 622-633; b) J. Kondo, Y. Tada, T. Dairaku, Y. Hattori, H. Saneyoshi, A. Ono, Y. Tanaka, *Nat. Chem.* **2017**, *9*, 956-960; c) S. M. Swasey, E. G. Gwinn, *New J. Phys.* **2016**, *18*, 045008; d) S. Hensel, K. Eckey, P. Scharf, N. Megger, U. Karst, J. Müller, *Chem. Eur. J.* **2017**, *23*, 10244-10248; e) F. Linares, E. García-Fernández, F. J. López-Garzón, M. Domingo-García, A. Orte, A. Rodríguez-Diéguez, M. A. Galindo, *Chem. Sci.* **2019**, *10*, 1126-1137; f) L. Mistry, O. El-Zubir, G. Dura, W. Clegg, P. G. Waddell, T. Pope, W. A. Hofer, N. G. Wright, B. R. Horrocks, A. Houlton, *Chem. Sci.* **2019**, *10*, 3186-3195.

[5] a) B. Lippert, P. J. Sanz Miguel, *Acc. Chem. Res.* **2016**, *49*, 1537–1545; b) N. Zimmermann, E. Meggers, P. G. Schultz, *J. Am. Chem. Soc.* **2002**, *124*, 13684–13685; c) Y. Takezawa, M. Shionoya, *Acc. Chem. Res.* **2012**, *45*, 2066–2076; d) A. Ono, H. Torigoe, Y. Tanaka, I. Okamoto, *Chem. Soc. Rev.* **2011**, *40*, 5855–5866; e) P. Scharf, J. Müller, *ChemPlusChem* **2013**, *78*, 20–34; f) H. Mei, I. Röhl, F. Seela, *J. Org. Chem.* **2013**, *78*, 9457-9463; g) S. K. Jana, X. Guo, H. Mei, F. Seela, *Chem. Commun.* **2015**, *51*, 17301-17304; h) H. Mei, S. A. Ingale, F. Seela, *Chem. Eur. J.* **2014**, *20*, 16248-16257; i) H. Zhao, P. Leonard, X. Guo, H. Yang, F. Seela, *Chem. Eur. J.* **2017**, *23*, 5529-5540; j) J. M. Méndez-Arriaga, C. R. Maldonado, J. A. Dobado, M. A. Galindo, *Chem. Eur. J.* **2018**, *24*, 4583-4589; k) A. Ono, S. Cao, H. Togashi, M. Tashiro, T. Fujimoto, T. Machinami, S. Oda, Y. Miyake, I. Okamoto, Y. Tanaka, *Chem. Commun.* **2008**, 4825-4827.

[6] X. Guo, P. Leonard, S. A. Ingale, J. Liu, H. Mei, M. Sieg, F. Seela, *Chem. Eur. J.* **2018**, *24*, 8883-8892.

[7] S.-H. Kim, D. G. Bartholomew, L. B. Allen, *J. Med. Chem.* **1978**, *21*, 883-889; b) H. Rosemeyer, F. Seela, *J. Org. Chem.* **1987**, *52*, 5136-5143; c) F. Seela, H. Rosemeyer, 5-Aza-7-deazapurines: Synthesis and Properties of Nucleosides and Oligonucleotides, in *Recent Advances in Nucleosides: Chemistry and Chemotherapy* (Ed. D. C. K. Chu), Elsevier Press,

Amsterdam **2002**, 505-533; d) L. Zhang, Z. Yang, K. Sefah, K. M. Bradley, S. Hoshika, M.-J. Kim, H.-J. Kim, G. Zhu, E. Jiménez, S. Cansiz, I.-T. Teng, C. Champanhac, C. McLendon, C. Liu, W. Zhang, D. L. Gerloff, Z. Huang, W. Tan, S. A. Benner, *J. Am. Chem. Soc.* **2015**, *137*, 6734–6737; e) M. M. Georgiadis, I. Singh, W. F. Kellett, S. Hoshika, S. A. Benner, N. G. J. Richards, *J. Am. Chem. Soc.* **2015**, *137*, 6947–6955; f) F. Seela, S. Amberg, A. Melenewski, H. Rosemeyer, *Helv. Chim. Acta* **2001**, *84*, 1996-2014; g) Z. Yang, D. Hutter, P. Sheng, A. M. Sismour, S. A. Benner, *Nucleic Acids Res.* **2006**, *34*, 6095-6101; h) F. Seela, A. Melenewski, *Eur. J. Org. Chem.* **1999**, 485-496.

[8] a) X. Guo, F. Seela, *Chem. Eur. J.* **2017**, *23*, 11776-11779; b) S. L. Müller, X. Zhou, P. Leonard, O. Korzhenko, C. Daniliuc, F. Seela, *Chem. Eur. J.* **2019**, *25*, 3077-3090.

[9] M. Hoffer, *Chem. Ber.* **1960**, *93*, 2777-2781.

[10] a) M. Fortino, T. Marino, N. Russo, *J. Phys. Chem. A* **2015**, *119*, 5153-5157; b) T. J. Kistenmacher, M. Rossi, L. G. Marzilli, *Inorg. Chem.* **1979**, *18*, 240-244.

[11] J. A. McDowell, D. H. Turner, *Biochemistry* **1996**, *35*, 14077–14089.

[12] a) G. Rosetti, P. D. Dans, I. Gomez-Pinto, I. Ivani, C. Gonzalez, M. Orozco, *Nucleic Acids Res.*, **2015**, *43*, 4309-4321; b) N. Sugimoto, M. Nakano, S-i. Nakano, *Biochemistry* **2000**, *39*, 11270-11281; c) P. Modrich, *Ann. Rev. Biochem.* **1987**, *56*, 435-466; d) J. SantaLucia Jr., D. Hicks, *Ann. Rev. Biophys. Biomol. Struct.* **2004**, *33*, 415-440; e) S. Ebel, A. N. Lane, T. Brown, *Biochemistry* **1992**, *31*, 12083-12086.

[13] a) L. A. E. Leal, A. Karpenko, S. Swasey, E. G. Gwinn, V. Rojas-Cervellera, C. Rovira, O. Lopez-Acevedo, *J. Phys. Chem. Lett.* **2015**, *6*, 4061-4066; b) A. Terrón, B. Moreno-Vachiano, A. Bauzá, A. García-Raso, J. J. Fiol, M. Barceló-Oliver, E. Molins, A. Frontera, *Chem. Eur. J.* **2017**, *23*, 2103-2108.

[14] M. Frisch, G. Trucks, H. B. Schlegel, G. Scuseria, M. Robb, J. Cheeseman, G. Scalmani, V. Barone, B. Mennucci, G. E. Petersson, Gaussian 09, Gaussian, Inc, Wallingford, CT **2009**.

[15] S. L. Mayo, B. D. Olafson, W. A. Goddard, *J. Phys. Chem.* **1990**, *94*, 8897-8909.

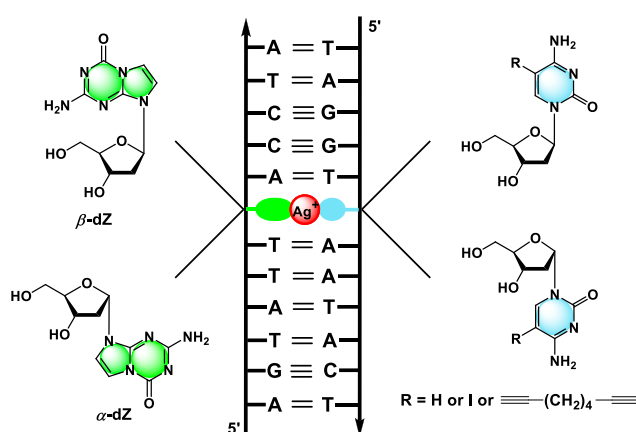
[16] M. Frisch, J. A. Pople, J. S. Binkley, *J. Chem. Phys.* **1984**, *80*, 3265-3269.

[17] P. J. Hay, W. R. Wadt, *J. Chem. Phys.* **1985**, *82*, 299-310.

Table of contents entry

Anomeric 5-Aza-7-deaza-2'-deoxyguanosines in Silver Ion Mediated Homo and Hybrid Base Pairs: Impact of Mismatch Structure, Helical Environment and Nucleobase Substituents on DNA Stability

Xinglong Zhou, Dasharath Kondhare, Peter Leonard, and Frank Seela*



Silver-mediated base pairing in DNA: Silver-mediated α/α and β/β homo base pairs formed by anomeric 5-aza-7-deaza-2'-deoxyguanosine and 2'-deoxycytidine residues are more stable than α/β hybrid pairs. This is different to silver-mediated dC-dC pairs in which the α/β hybrid pairs were the most stable structures. Positional change of base pairs in duplex DNA alters silver-mediated base pair stability, whereas functionalization of the base pair has a minor impact.